



U.S. DEPARTMENT OF
ENERGY

Office of
Science

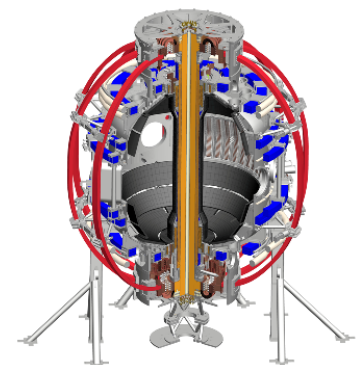


Operational characteristics and non-inductive plasmas on NSTX-U*

D. Mueller¹, D.J. Battaglia¹, M.D. Boyer¹, W. Guttenfelder¹,
C.E. Myers¹, F.M. Poli¹, R. Raman² and NSTX-U Team

¹PPPL ²Univ. Of Washington

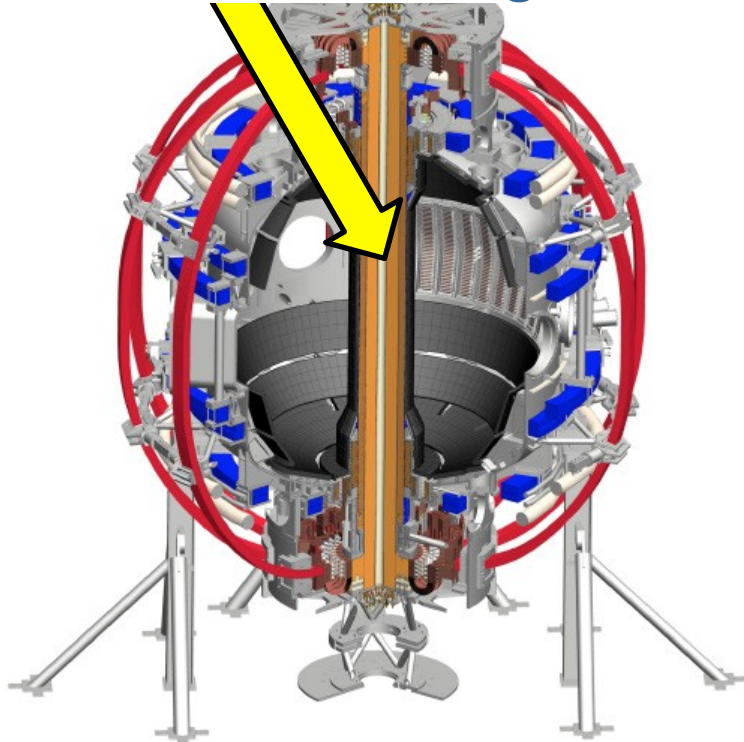
58th Annual APS-DPP Meeting
San Jose, CA
October 21- November 4, 2016



*Work supported by US DOE Contract No. DE-AC02-09CH11466

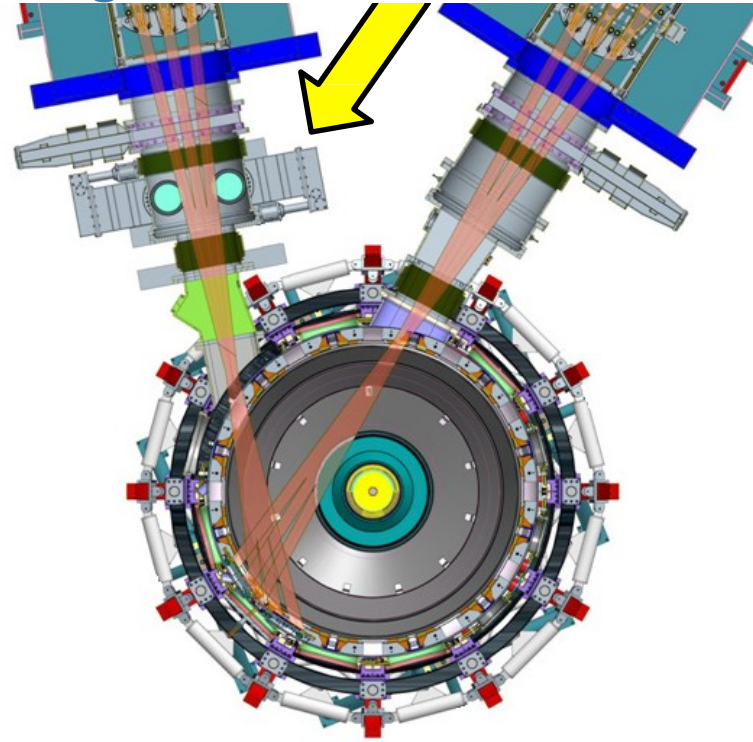
NSTX-U will access new physics with 2 major new tools:

1. New Central Magnet



Higher T, low v^* from low to high β
→ Unique regime, study new transport and stability physics

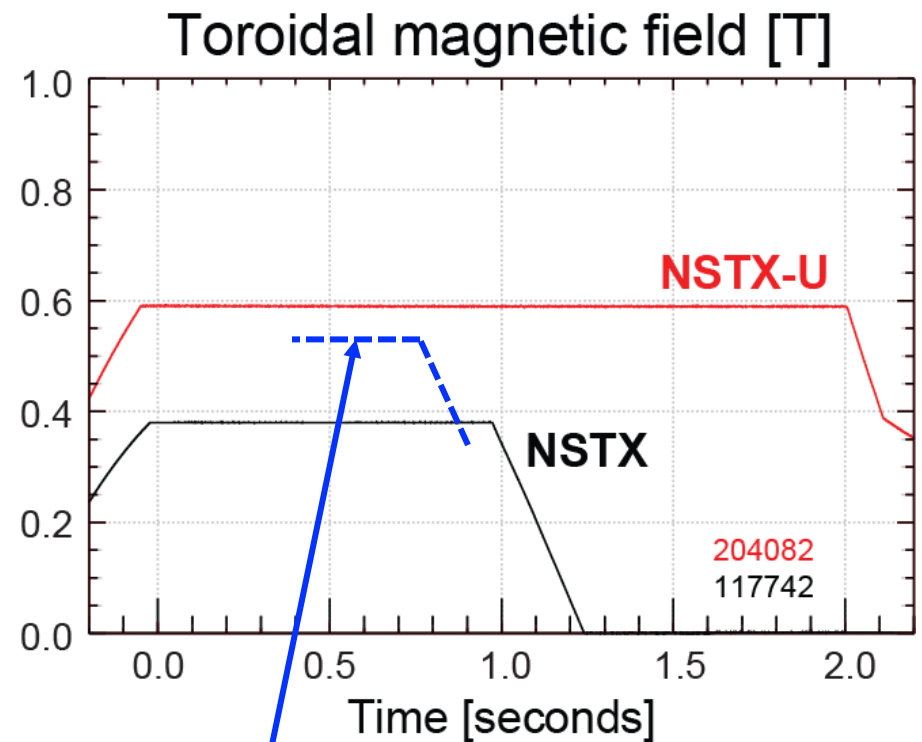
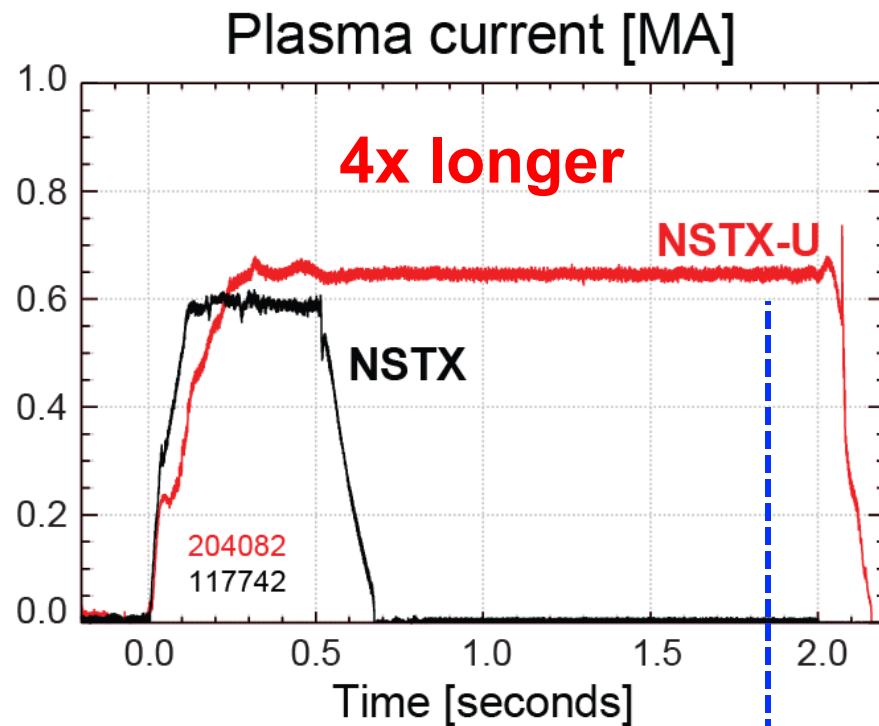
2. Tangential 2nd Neutral Beam



Full non-inductive current drive
→ Not demonstrated in ST at high- β_T
Essential for any future steady-state ST

NSTX-U surpassed maximum pulse duration and magnetic field of NSTX

Compare similar **NSTX** / **NSTX-U** Boronized L-modes, $P_{\text{NBI}}=1\text{MW}$



NSTX-U L-mode duration exceeds longest NSTX H-mode

NSTX-U B_T > highest NSTX B_T

$n=1$ error field correction (EFC) optimized to maximize pulse length, discharge performance

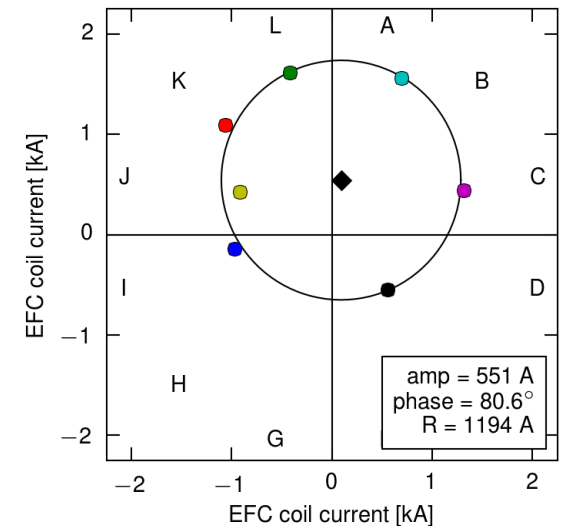
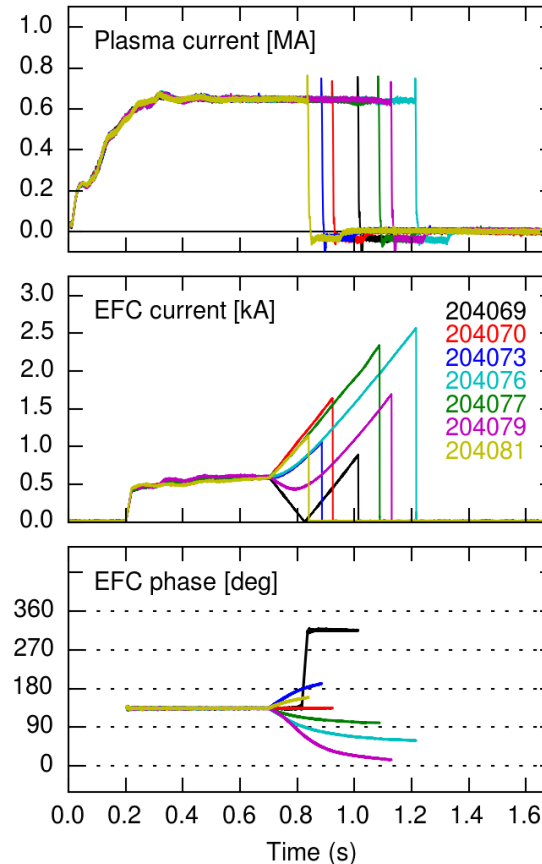
Compass scan steps:

1. Select $n=1$ phase
2. Ramp $n=1$ amplitude until the discharge terminates
3. Repeat at multiple phases
4. Fit circle to locking points
5. The optimum EFC is located at the center of the circle

Optimum EFC:

- $\phi = 80^\circ$
- $I_{\text{EFC}} = 550$

L-Mode Plasmas

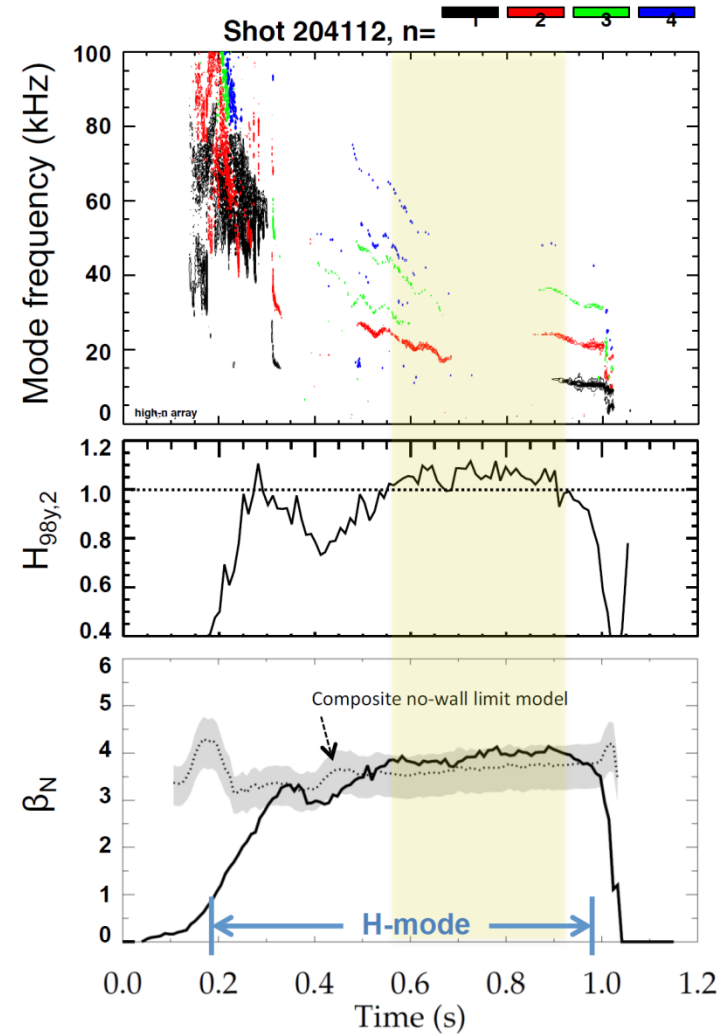
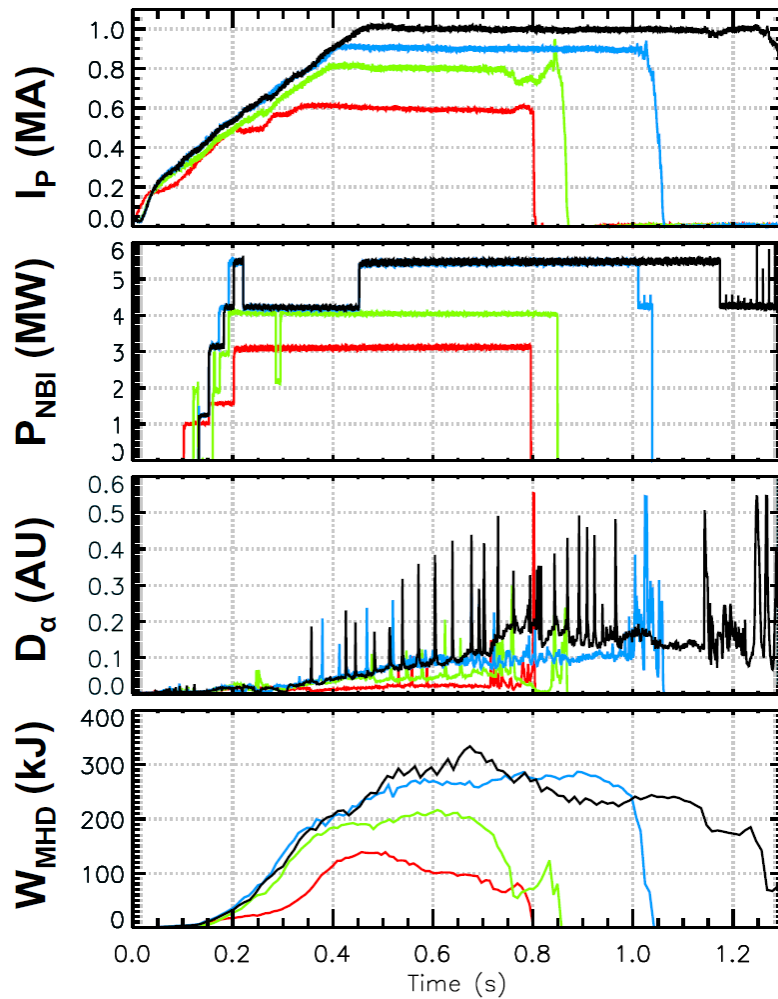


- Six independently controllable window pane coils centered on the mid-plane
- Window pane coils can apply a static $n=1$ error correction field
- Further $n=1$ work: error field is different during ramp-up, diagnose and correct

Recovered ~1MA H-modes with weak/no core MHD

202946 – no EFC 204112 – EFC v2
 203679 – EFC v1 204118 – EFC v2

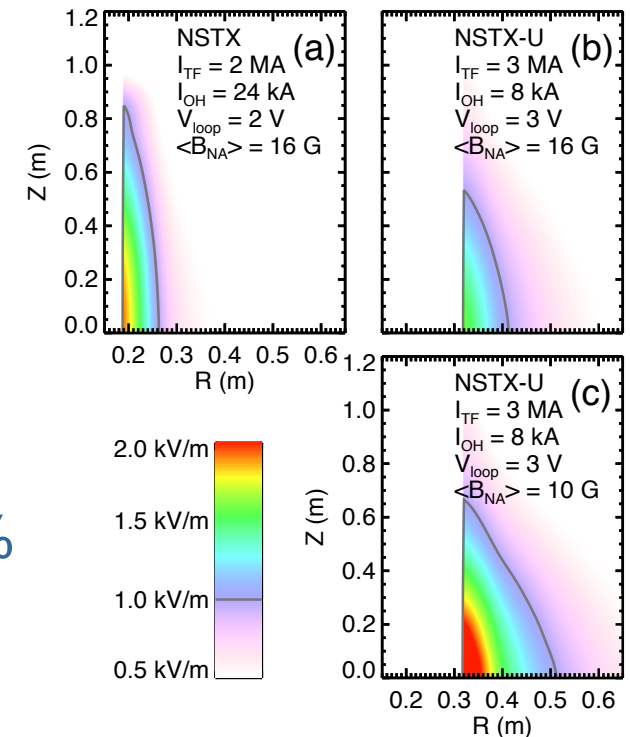
$H_{98} \geq 1$, $\beta_N \geq n=1$ no-wall limit



Start-up and ramp-up phases

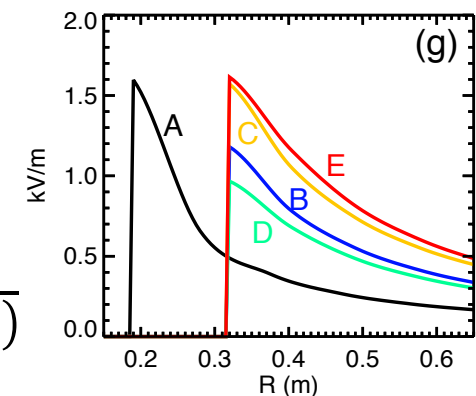
Breakdown successful at lower V_{loop} than anticipated from calculations for NSTX-U

- Smaller V_{loop} needed for breakdown compared to model predictions
 - 8 kA OH precharge: $V_{loop} \sim 3V$ (first 2 ms)
 - Model predicted $V_{loop} \sim 4V$
 - Scales to $V_{loop} = 2 V$ at $B_T = 1T$
 - Model matches experiment if the 3D error field near inboard midplane reduced $\sim 40\%$
 - Consistent with smaller OH x TF tilting



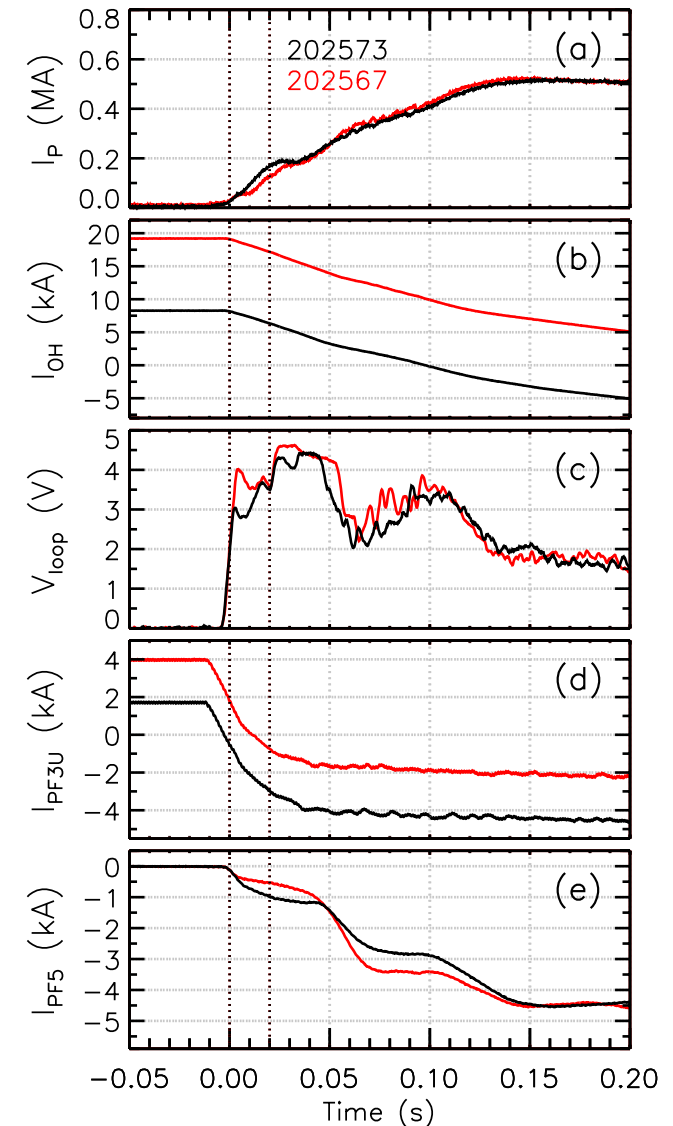
- Breakdown region has smaller Z , larger R extent compared to NSTX, consistent with model

$$\frac{V_{loop} I_{TF}}{\pi R^2 (B_\theta + \langle B_{\theta,NA} \rangle)}$$

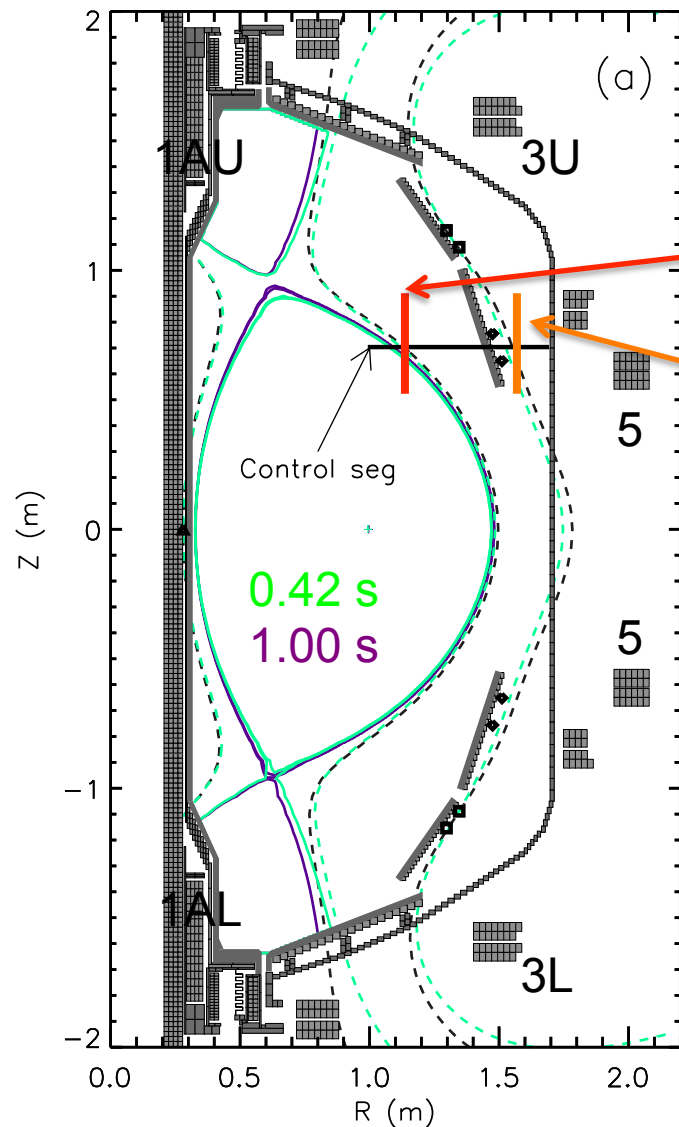


Breakdown LRDFIT calculations led to viable startup scenarios at two OH precharge levels

- Larger V_{loop} needed with larger ohmic precharge
 - Size of field null reduced at larger I_{OH}
 - 25% increase in V_{loop} matches calculations comparing 8 and 20 kA cases
- 8 and 20 kA OH precharge routinely used
 - Both scenarios retained passive R and Z stability, and achieved > 100 kA by 20ms for transition to ramp-up
- Will develop a library of start-ups for other pre-charges



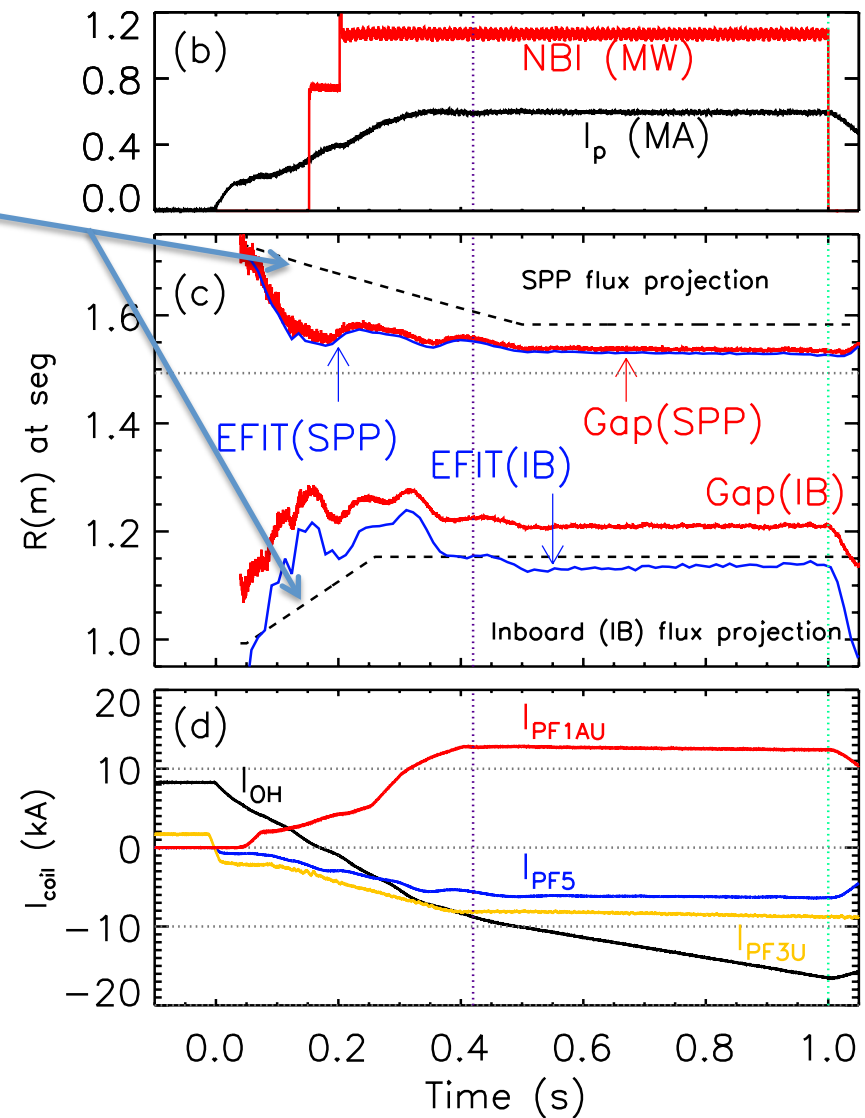
“Gap” plasma shape control used during ramp-up and ramp-down phases



- Outboard PF coils control the position of flux surfaces on a control segment
 - Flux surface at inboard midplane
 - Controls outer gap
 - Flux surface at secondary passive plate
 - Controls elongation
 - All calculations assume plasma is up-down symmetric
 - Flux along control segment assumed to vary linearly, constrained by measurements at the primary passive plate
- Divertor coils in relational control
 - $I_{PF} = A I_p + B I_{OH} + C$
 - Second term (“B”) compensates for changing OH fringe field

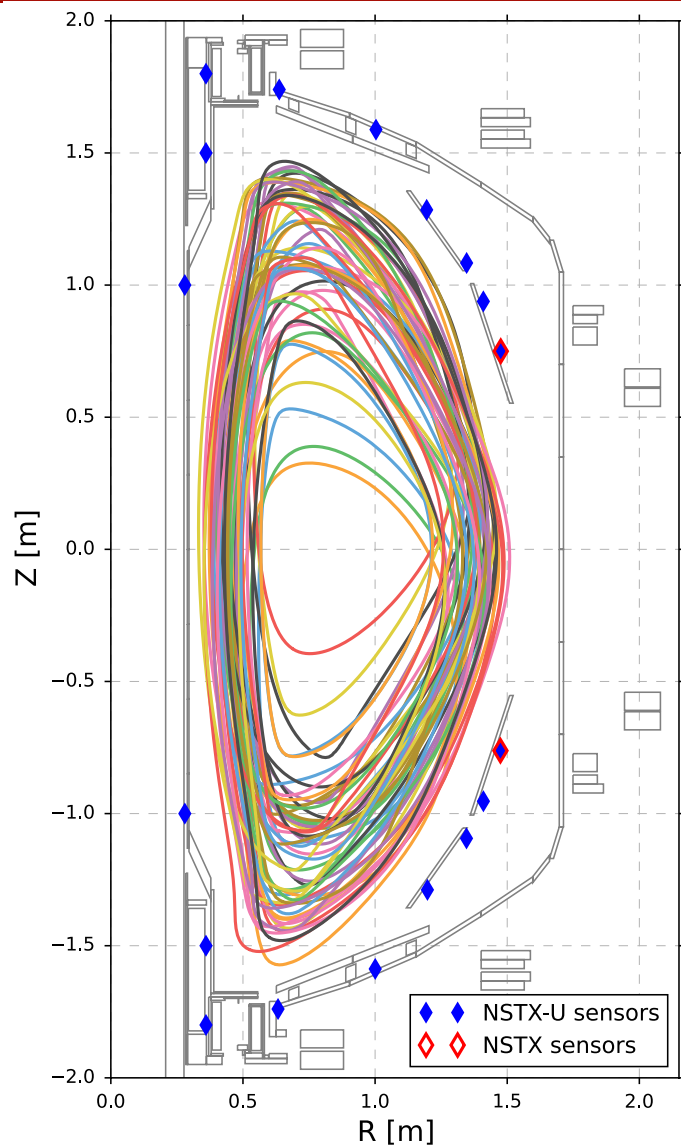
First L- and H-mode discharges on NSTX-U used Gap control for the entire discharge

- Dashed lines (c): requested position of two flux surfaces on control segment
- Red lines (c): flux surface position calculated by Gap math
 - Prop. gain only, always a finite error
- Blue lines (c): flux surface as calculated by offline EFIT
 - Difference from red lines due to assumptions in Gap calculation
- PF1A provides diverting field
 - Slight decrease in PF coil currents during flattop due to change OH fringe field

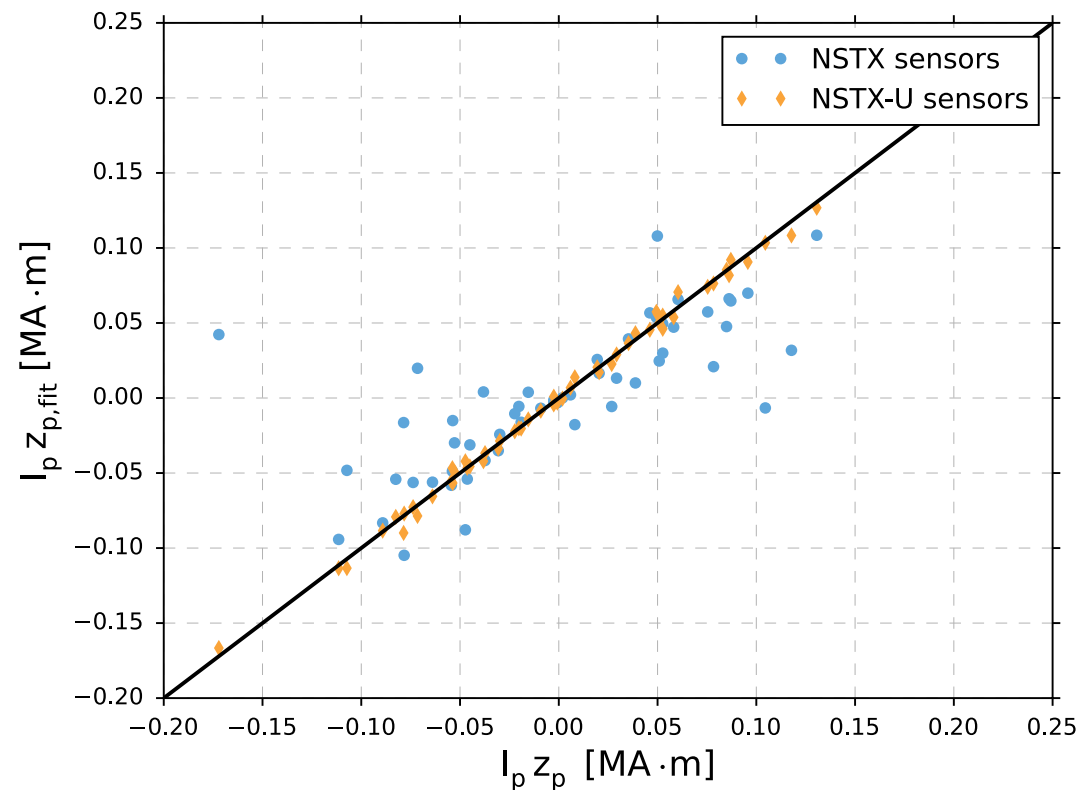


Plasma Control

Additional flux/voltage differences improved estimation of vertical position/velocity

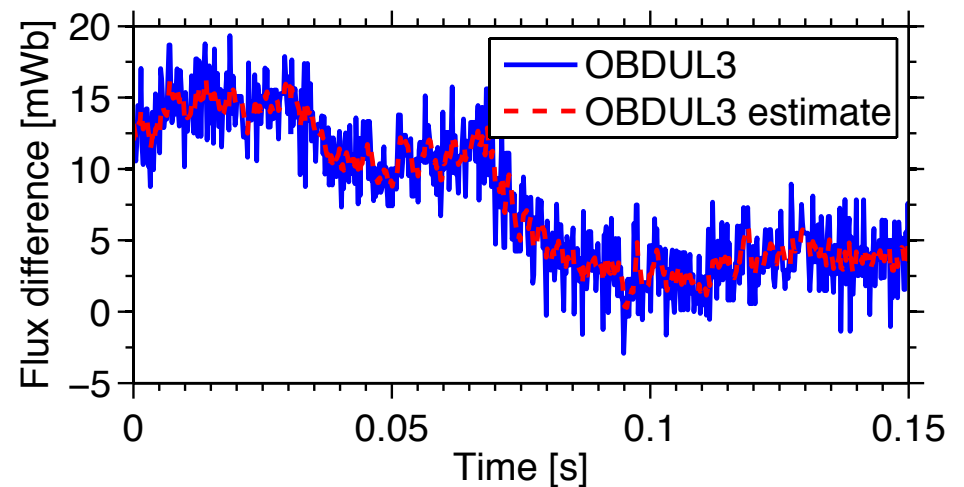
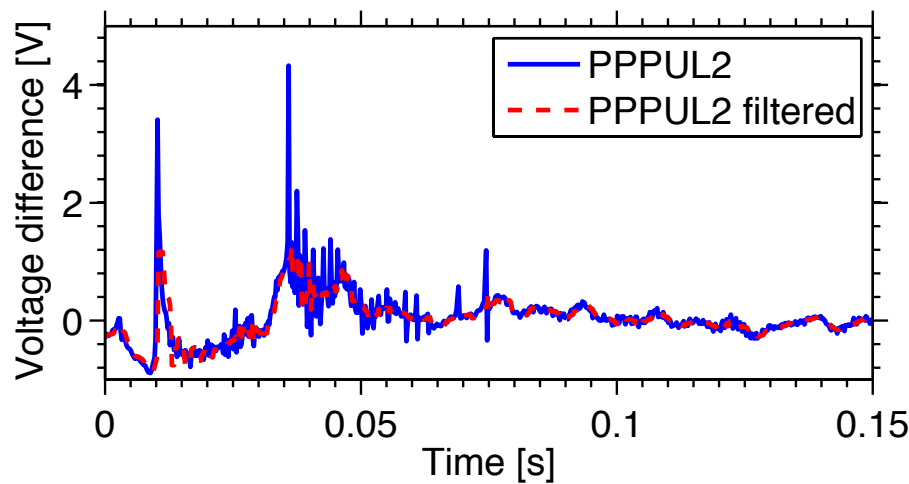
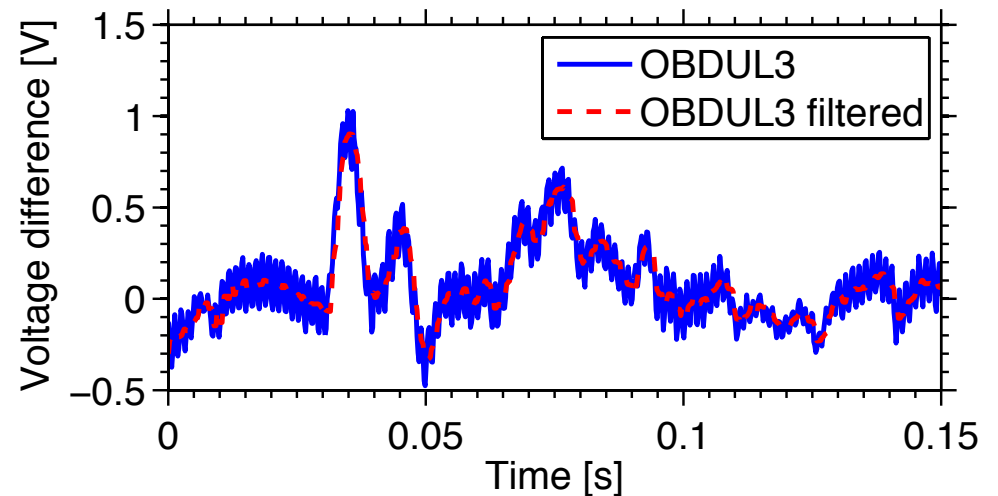


- ~60 NSTX-U equilibria generated with ISOLVER free boundary code
- Flux loop weights determined by **least squares fit to $I_p Z_p$**
- Optimal weights **adjusted based on EFIT reconstructions of experimental discharges**

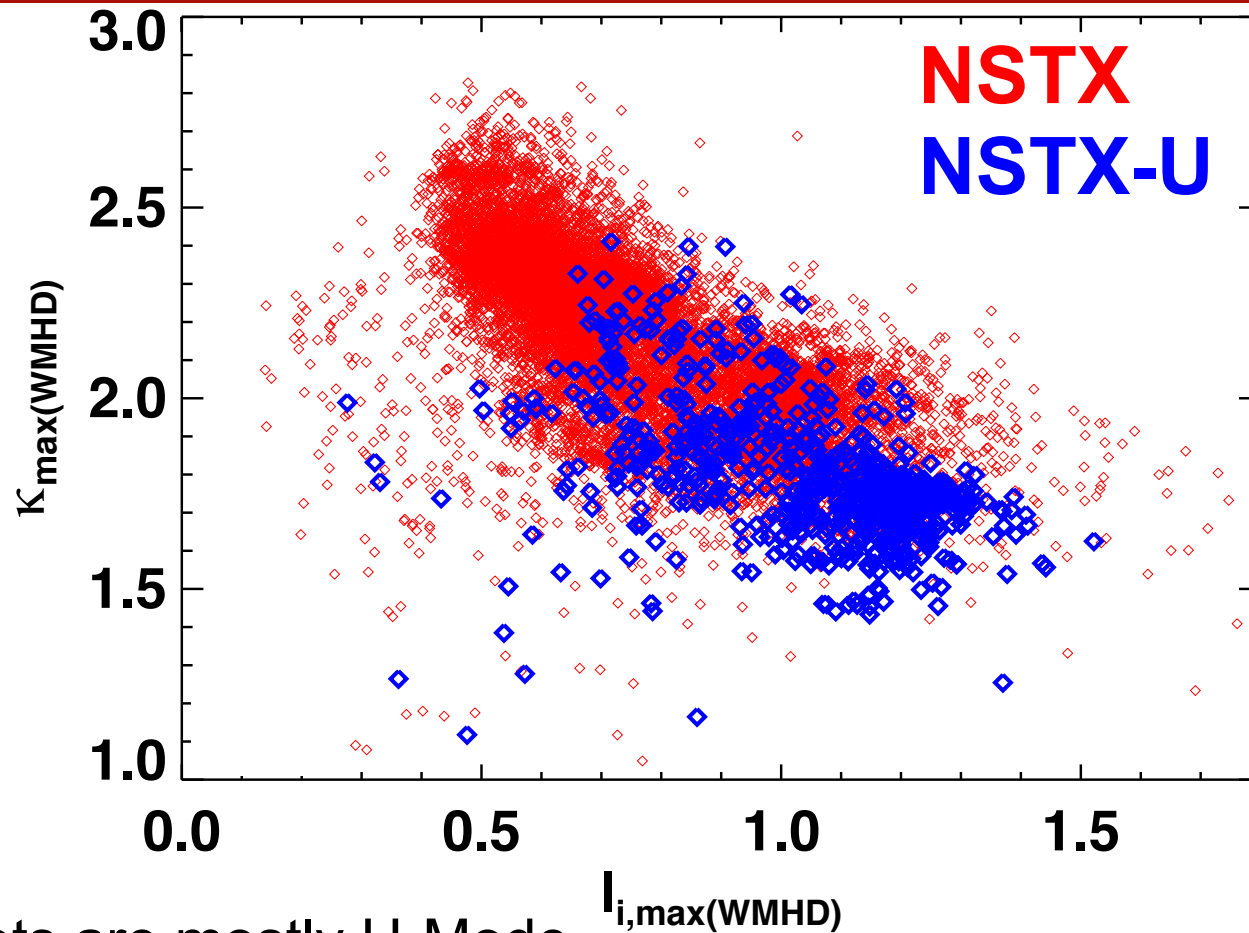


Filtering added to remove unwanted pick-up on vertical estimation sensors

- Voltage differences
 - power supply ripple and noise spikes Too fast for control system response
- Flux differences
 - Kalman filter used to estimate the flux differences



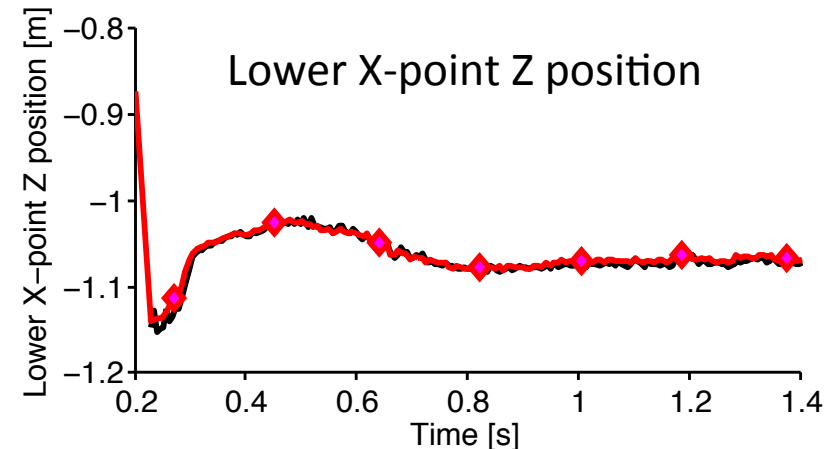
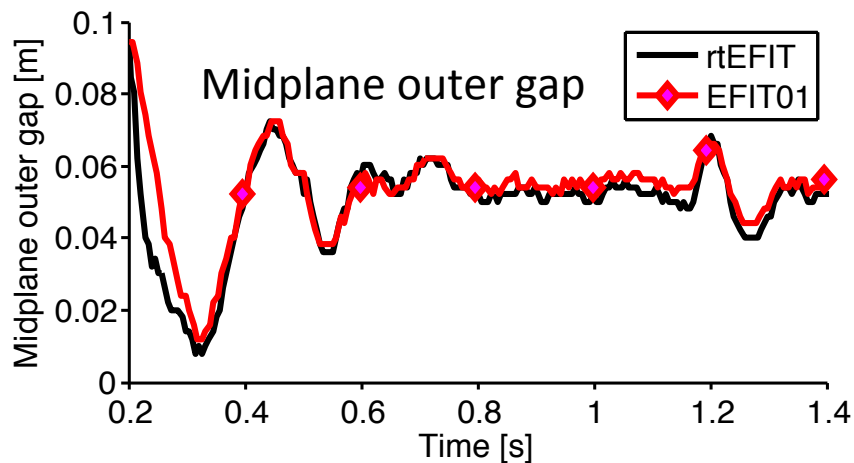
Improved vertical control allows NSTX-U to achieve elongation similar to lower aspect ratio NSTX



- NSTX shots are mostly H-Mode
- NSTX-U vertical control gains tuned during $I_i > 1$ operation
- Lower I_i shots in NSTX-U are H-modes

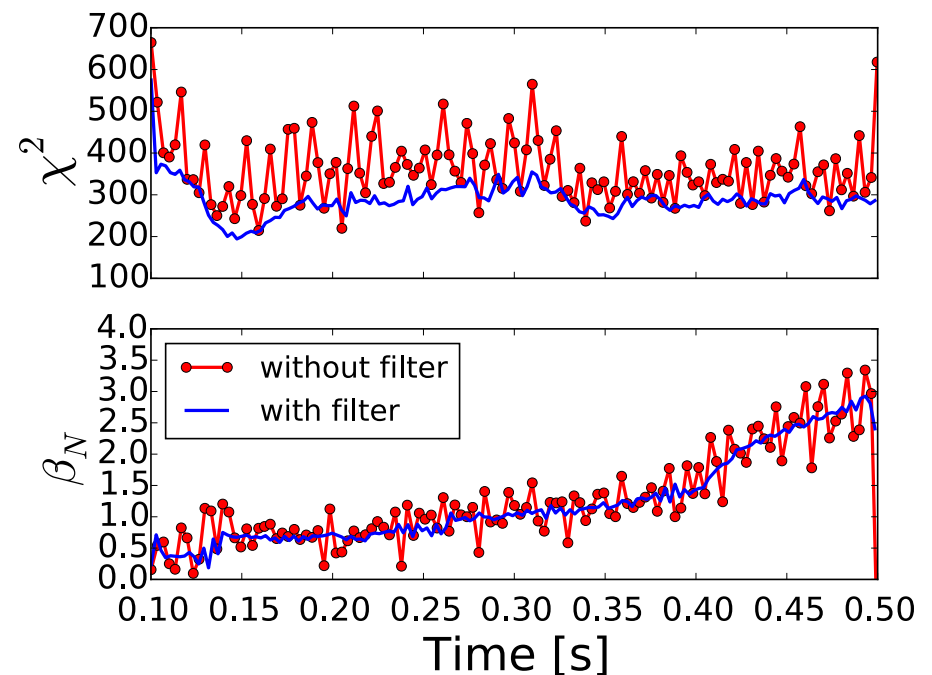
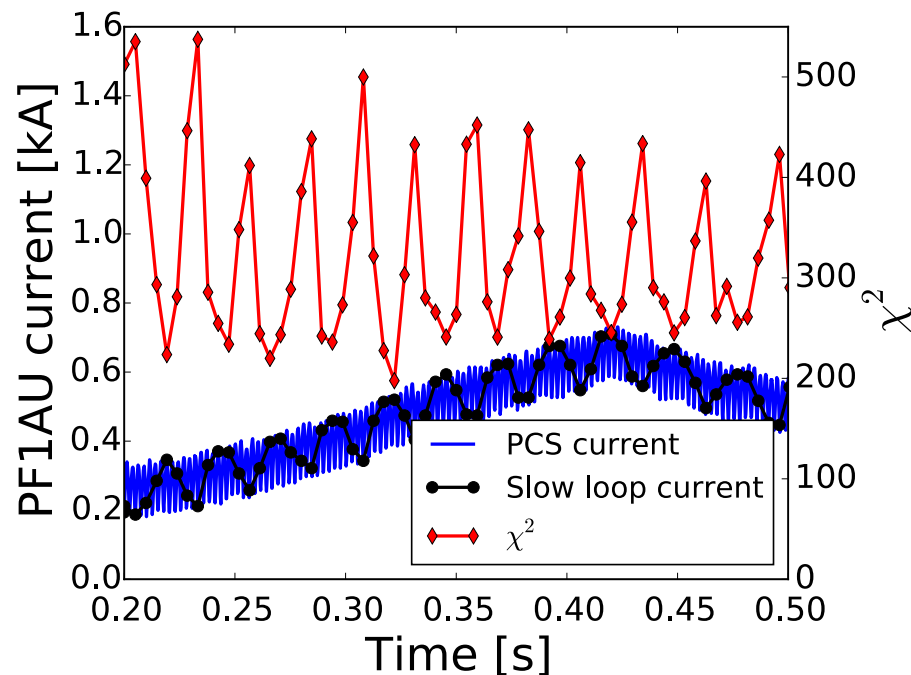
Updated and improved rtEFIT for real-time reconstruction on NSTX-U

- Updated grid size to 65x65 (from 33x33) and vessel/coil model
- Tested using TRANSP data prior to run, rt4 early on
- Multi-threading enabled more complex calculations
 - β_N , I_j , q calculated in real-time
 - Coil and vessel currents fit instead of treated as known
- Calculated gaps and X-point positions match closely to offline magnetics-only EFIT (EFIT01)



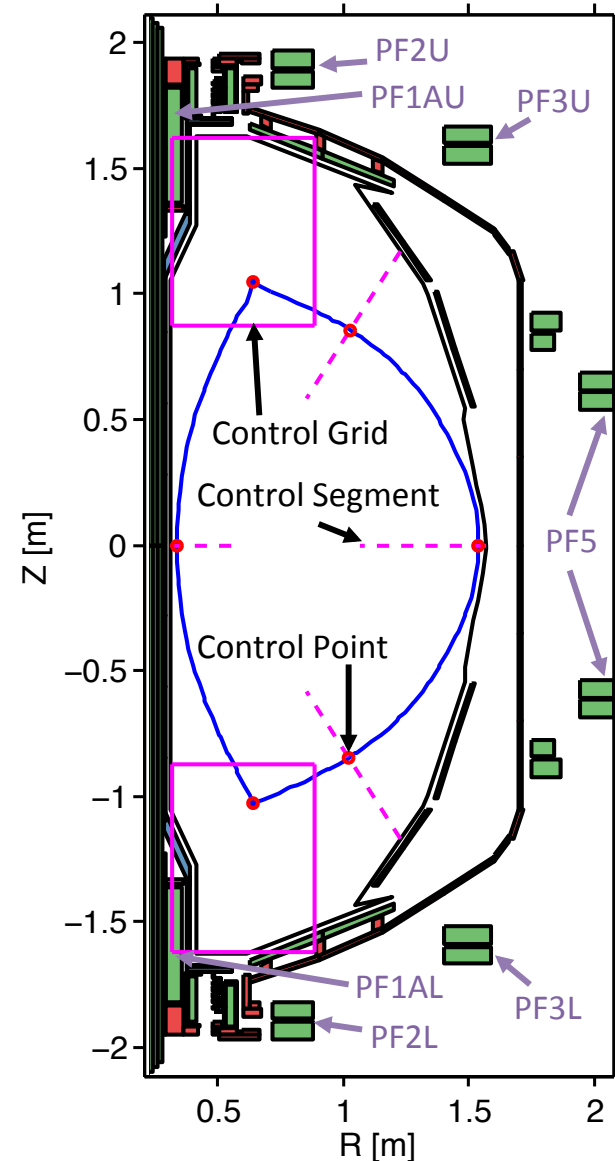
Anti-aliasing filter fixed fits due to PF1A power supply ripple

- Aliasing of power supply ripple on slow loop time scale caused poor fitting, oscillations
- rtEFIT fast and slow loops
 - **Fast** (every PCS cycle time): determines **flux at control points** based on last reconstruction and new diagnostics
 - **Slow** (~5-25 PCS cycle times): single iteration **reconstruction**

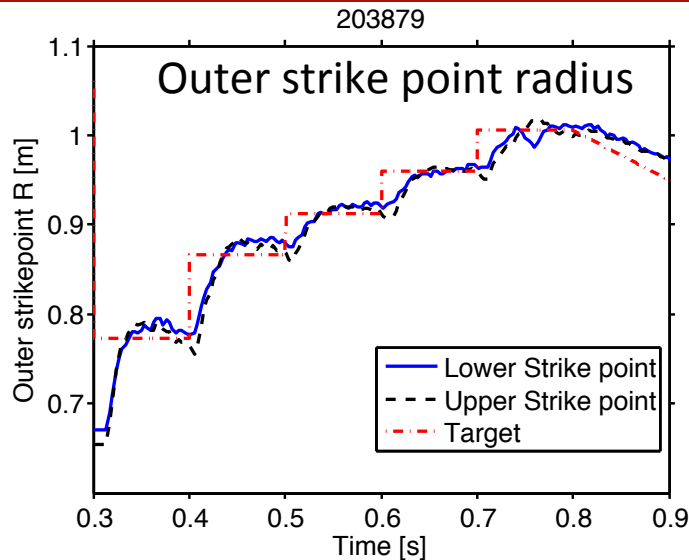


ISOFLUX shape control on NSTX-U

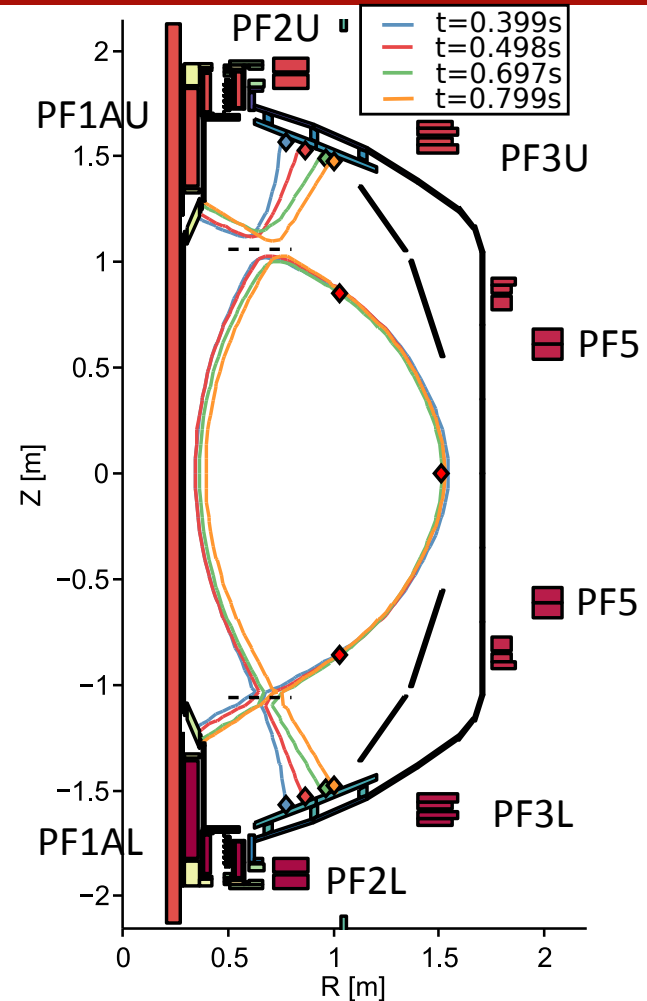
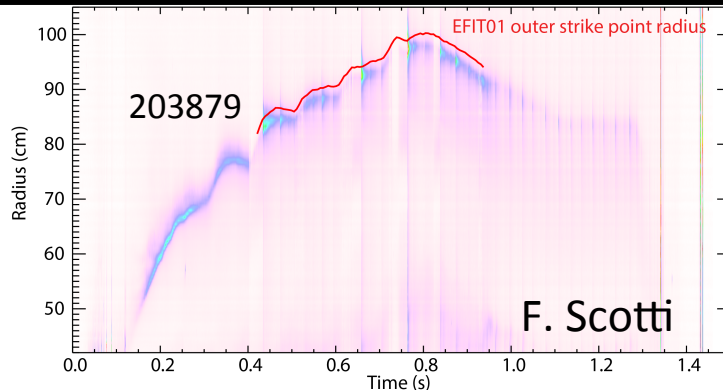
- Control points are the intersection of control segments with the target boundary
- Two main algorithms:
 - ISOELONG – inner wall limited discharges
 - ISODNULL – diverted discharges
- Total re-write of code by K. Erickson
 - 75% reduction in # lines of code
 - Makes changing/adding functionality much easier



ISODNULL used to control the location of the outer strike points



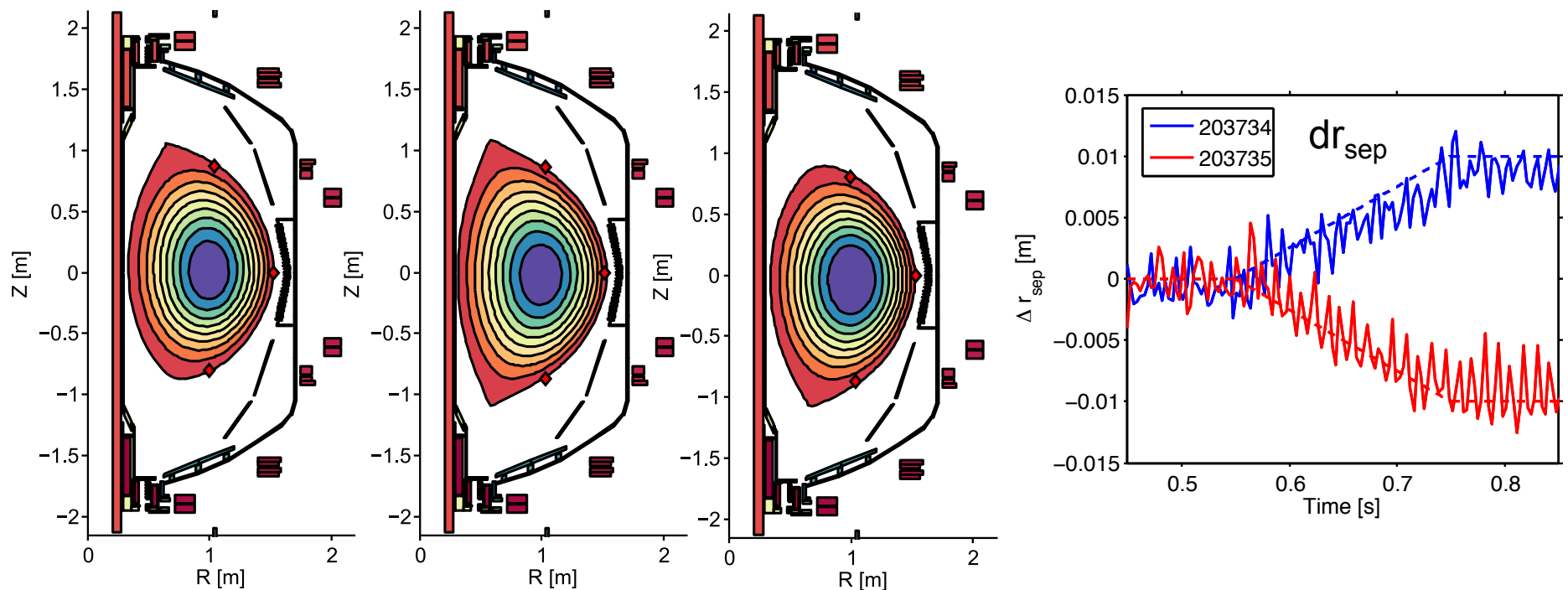
Lower divertor outer strike-point C II emission



- Demonstrated ability to scan the outer strike point location with the X-point height and outer gaps fixed using PF1A and PF2s

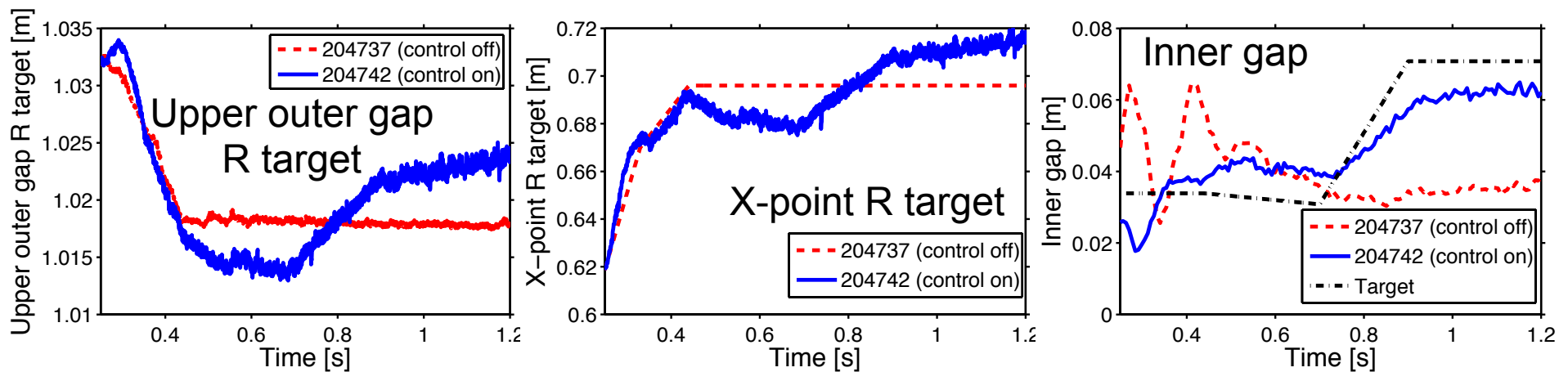
Control of dr_{sep}

- dr_{sep} is the midplane radial distance between the upper and lower X-point fluxes
- Controlled by adjusting the upper and lower-outer gap control point locations in real-time



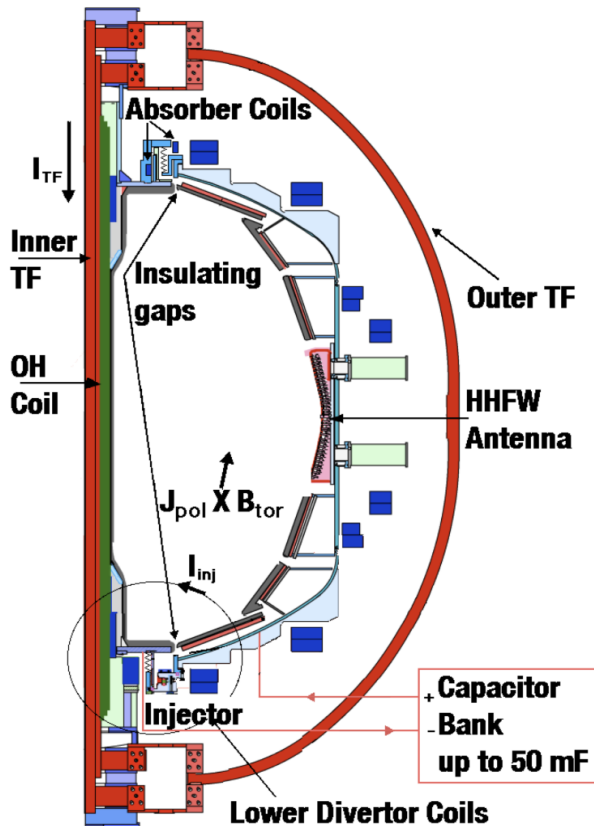
A novel method of inner gap control has been tested

- No shaping coils on inboard side, available coils already assigned...
 - No way to independently control the inner gap
- Approach:
 - Automatically adjust other shaping parameters based on operator provided weight matrix to achieve desired inner gap

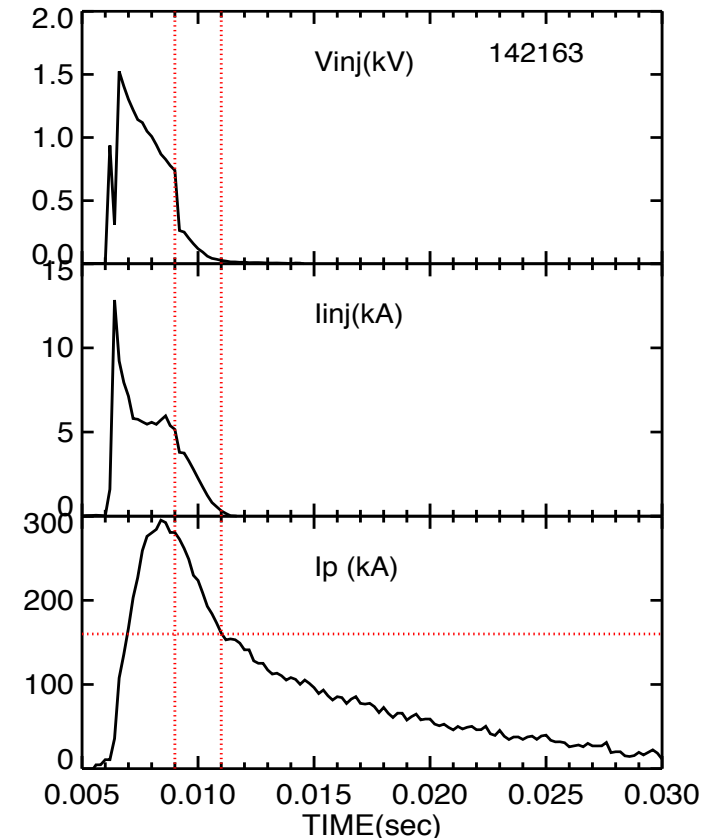


Non-inductive plasma plans

Coaxial Helicity Injection (CHI) initiation produces 100's of kA in cold plasma

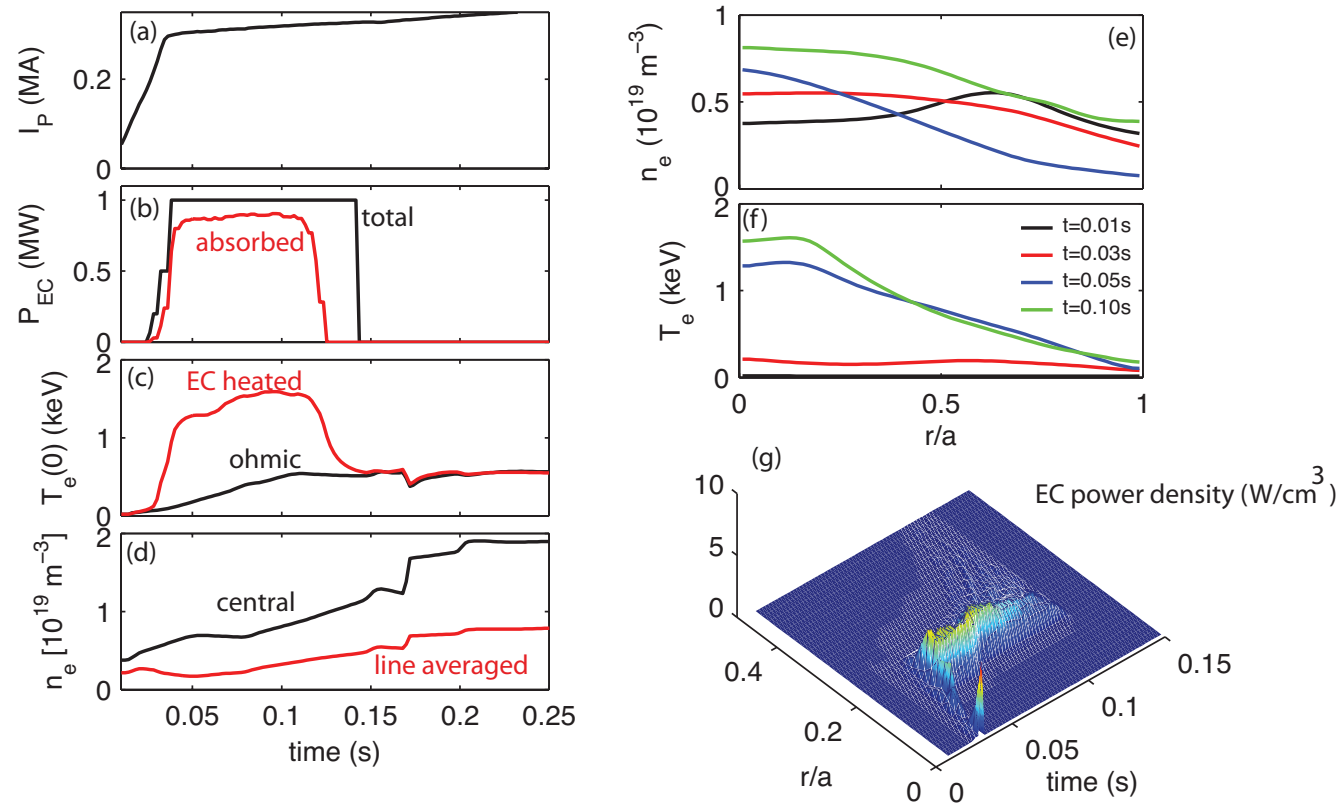


• CHI discharge using 30 mF at 1.46 kV.



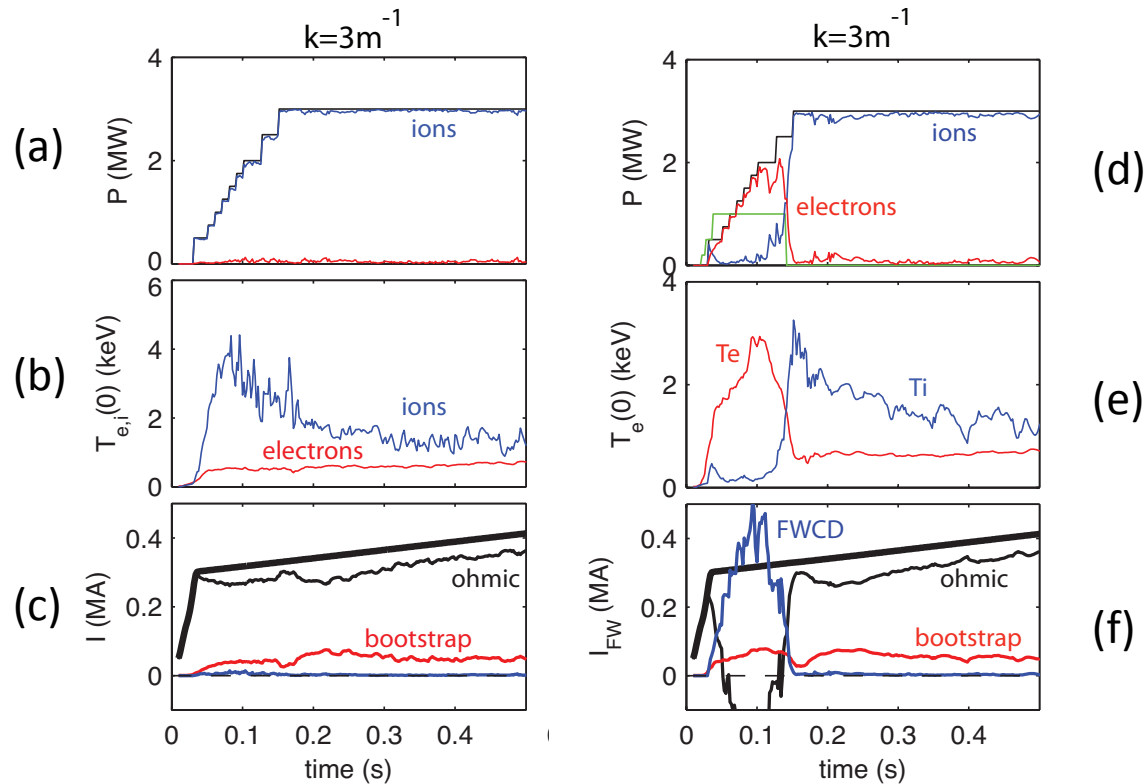
- The injector current decays after the crowbar is fired and is zero at 11 ms.
- The toroidal current is 280 and 160 kA at 9 and 11 ms respectively.
- A relatively long decay time of the toroidal current is achieved only when impurities are controlled.

Electron Cyclotron Heating (ECH) heats CHI initiated plasmas



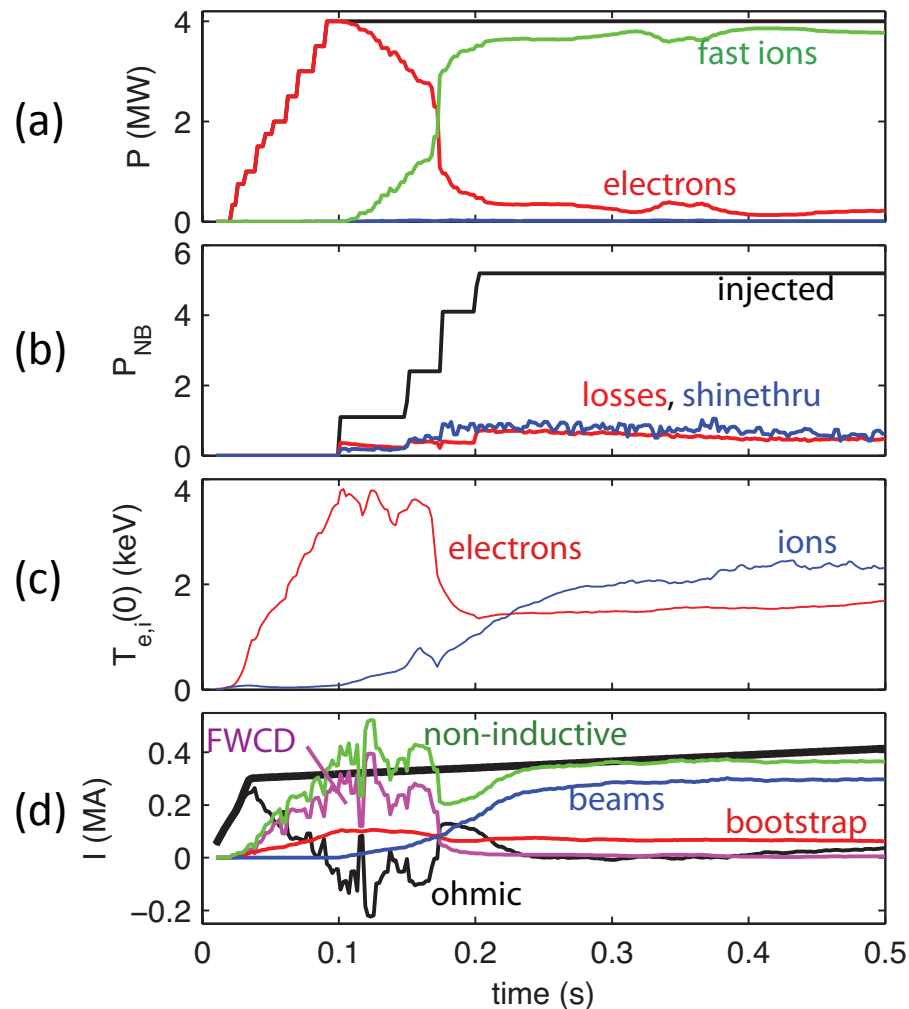
Simulation of EC heating. Left panel: time traces of (a) plasma current, (b) injected and absorbed power, (c) electron temperature on axis compared with an ohmic plasma, (d) central and line-averaged density. Right panel: profiles of (e) electron density (f) electron temperature and (g) EC heating profile.

High Harmonic Fast Waves (HHFW) drive current at low density for T_e is >1 keV



Comparison of two simulations without (left) and with EC heating (right) for parallel wavenumber of $k_{||} = 3 \text{ m}^{-1}$. (a) Injected power and power absorbed by the ions and the electrons. (b) central value of electron and ion temperature (c) total current waveform and contributions: ohmic (black), FWCD (blue), bootstrap (red).

At higher density HFW less effective NBI ramps-up plasma current.



Simulations with EC, HFW and NBI at start-up (a) HFW injected power and power absorbed to the electrons (red) and to the fast ions (green). (b) Neutral Beam injected (black) power, and absorbed by the electrons (red) and by the ions (blue). (c) Central value of electron and ion temperature. (d) current waveform (thick black) and contributions: FWCD (magenta), beam current (blue), ohmic (black) and bootstrap (red), the total non-inductive current is also shown for comparison (green).